CORRECTED 11 APRIL 2008; SEE LAST PAGE

Foundation scholarship to C.G.; by a Grant-in-Aid for Young Scientists (B) (19770035) from the Ministry of Education, Culture, Sports, Science and Technology (MEXT) of Japan to H.K.; by Grants-in-Aid for Scientific Research (B) (19370023) from MEXT of Japan to K.K.; and by a Grant-in-Aid to the John Innes Centre and a Biotechnology and Biological Sciences Research Council grant (BBS/B/04498) to L.D.

Supporting Online Material
www.sciencemag.org/cgi/content/full/319/5867/1241/DC1
Materials and Methods
Figs. S1 to S4
Tables S1 and S2
References

2 November 2007; accepted 22 January 2008
10.1126/science.1152505

Ceramide Triggers Budding of Exosome Vesicles into Multivesicular Endosomes

Katarina Trajkovic,[1,2*] Chieh Hsu,[1,2*] Salvatore Chiantia,[5] Lawrence Rajendran,[6] Dirk Wenzel,[3] Felix Wieland,[4] Petra Schwille,[5] Britta Brügger,[4] Mikael Simons[1,2,7]†

Intraluminal vesicles of multivesicular endosomes are either sorted for cargo degradation into lysosomes or secreted as exosomes into the extracellular milieu. The mechanisms underlying the sorting of membrane into the different populations of intraluminal vesicles are unknown. Here, we find that cargo is segregated into distinct subdomains on the endosomal membrane and that the transfer of exosome-associated domains into the lumen of the endosome did not depend on the function of the ESCRT (endosomal sorting complex required for transport) machinery, but required the sphingolipid ceramide. Purified exosomes were enriched in ceramide, and the release of exosomes was reduced after the inhibition of neutral sphingomyelinases. These results establish a pathway in intraendosomal membrane transport and exosome formation.

After endocytosis, proteins and lipids that are destined for lysosomal degradation are first incorporated into intraluminal vesicles (ILVs) of multivesicular endosomes (MVEs) and delivered to lysosomes for digestion (*1*, *2*). Alternatively, MVEs can directly fuse with the plasma membrane, which leads to release of the ILVs to the extracellular environment as exosomes, where they function in a multitude of intercellular signaling processes (*3*–*5*). How proteins and lipids are sorted to these subsets of ILVs directed either for lysosomal degradation or for secretion as exosomes is unknown.

To address this issue, we studied the membrane trafficking of the proteolipid protein (PLP) in Oli-neu cells, a mouse oligodendroglial cell line that contains a large number of MVEs (*6*). To analyze whether PLP was released in association with exosomes, we subjected the cell culture medium of transiently transfected Oli-neu cells to sequential centrifugation steps with increasing centrifugal forces to obtain, finally, a 100,000*g* pellet, which mainly contained small membrane vesicles with a diameter of about 50 to 100 nm (Fig. 1B), similar to previously described exosomes (*3*–*5*). Relatively large amounts of PLP were found in the 100,000*g* pellet (Fig. 1A), and immunoelectron microscopy analysis revealed the presence of PLP on the vesicles (Fig. 1B). In contrast, PLP containing the cytotoxic, missense mutation [Val replaces Ala at position 242 (A242V); msd-PLP] that leads to misfolding of the protein and to retention in the endoplasmic reticulum (ER) was not detected in the 100,000*g* pellet (Fig. 1A); this finding excluded cell lysis as a major contributing factor. In addition, ER, Golgi, and early endosomal proteins and several exogenously expressed membrane proteins were not detected in the 100,000*g* pellet, which did contain the two exosomal proteins, Alix and flotillin (fig. S1) (*7*, *8*). In a continuous sucrose density gradient, the majority of PLP was enriched in the same fraction as the exosomal protein Alix (Fig. 1C). To explore whether PLP requires transport through the endosomal system to be released with exosomes, we cotransfected PLP with the early-endosomal guanosine triphosphatase–deficient Rab5 (Rab5^{Q79L}, in which Leu replaces Gln at position 79) to impair intraendosomal trafficking (*9*). Electron microscopy analysis of these endosomes revealed that they were filled with ILVs (fig. S2). A large fraction of PLP was

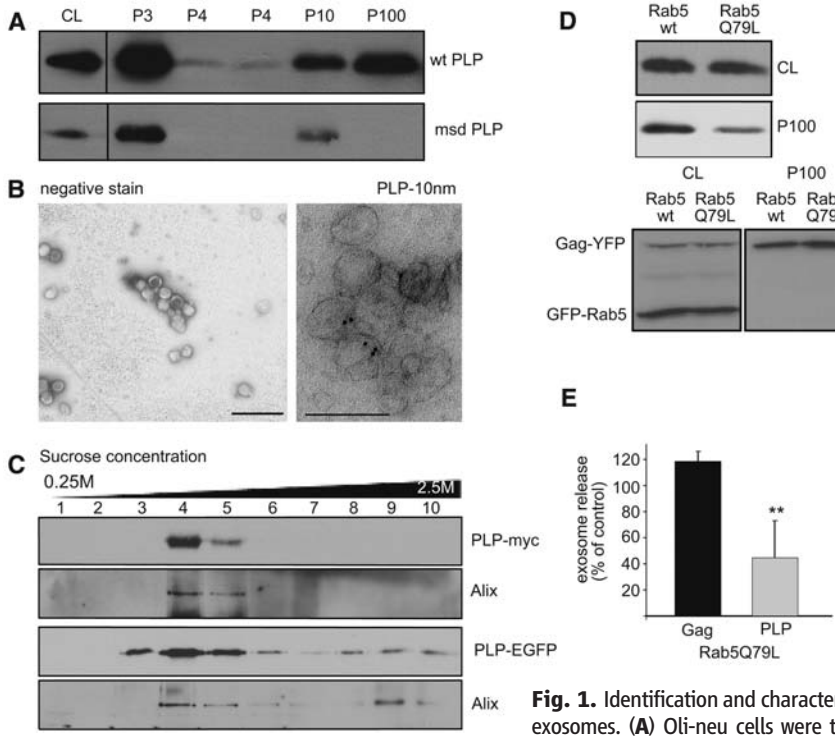

Fig. 1. Identification and characterization of exosomes. (**A**) Oli-neu cells were transiently transfected with Myc-tagged, wild-type (wtPLP) or mutant (msd-PLP) PLP; the medium was collected and submitted to sequential centrifugation steps as indicated. The resulting pellets of each centrifugation step were analyzed by Western blotting for PLP. (**B**) Cells were transiently transfected with PLP-Myc; 100,000*g* pellets were prepared and negatively stained with 1% uranyl acetate and immunolabeled with antibodies against PLP (right). Scale bar, 200 nm. (**C**) A 0.25 to 2.5 M sucrose gradient was loaded on top of the 100,000*g* pellet, and the resulting fractions were analyzed for PLP from transiently (PLP-Myc) or stably transfected (PLP-EGFP) cells and for the exosomal protein Alix. (**D** and **E**) Cells were cotransfected with either GFP-Rab5^{Q79L} or wild-type GFP-Rab5 (wt) and PLP-Myc or Gag-YFP; the amount of PLP and Gag in the cell lysates and 100,000*g* pellets was determined and quantified. Results are expressed as the mean ± SD of five experiments (**$P < 0.01$; one-sample *t* test against 100%).

[1]Centre for Biochemistry and Molecular Cell Biology, University of Göttingen, 37073 Göttingen, Germany. [2]Max-Planck-Institute for Experimental Medicine, 37075 Göttingen, Germany. [3]Max-Planck-Institute for Biophysical Chemistry, 37077 Göttingen, Germany. [4]Heidelberg University Biochemistry Center, 69120 Heidelberg, Germany. [5]BioTec, TU Dresden, 01307 Dresden, Germany. [6]Max-Planck-Institute of Cell Biology and Genetics, 01307 Dresden, Germany. [7]Department of Neurology, University of Göttingen, 37073 Göttingen, Germany.

*These authors contributed equally to this work.
†To whom correspondence should be addressed. E-mail: msimons@gwdg.de

entrapped in these enlarged endosomes, and the release of PLP with exosomes was significantly reduced (Fig. 1, D and E). The release from the plasma membrane of Moloney murine leukemia virus Gag fused to yellow fluorescent protein (Gag-YFP) with virus-like particles was not affected by Rab5^{Q79L}, which demonstrated the specificity of the effect (Fig. 1, D and E).

Thus, PLP-containing exosomes are derived from the endosomal system. How then is exosomal cargo segregated from nonexosomal cargo in endosomes? To study the possible segregation of cargo within distinct endosomal microdomains, we transfected cells with Rab5^{Q79L} to enlarge early endosomes and to facilitate domain inspection by confocal immunofluorescence analysis (*10*). Clathrin-coated microdomains on early endosomes contain the ubiquitin-binding protein Hrs, which sorts ubiquitinated proteins into these domains to mediate degradative protein sorting (*11*). To analyze whether PLP localized to these microdomains, we analyzed the localization of PLP in Rab5^{Q79L} enlarged endosomes. Little PLP colocalized with either Hrs or epidermal growth factor receptor (EGFR) (Fig. 2), whereas Hrs colocalized to a large extent with EGFR (fig. S3). The PLP-enriched domains colocalized with flotillin, a membrane scaffolding protein of lipid-raft microdomains, and with glycosylphosphatidylinositol fused to cyan fluorescent protein (GPI-CFP), which suggested that segregation of PLP from EGFR involves raft-based microdomains (Fig. 2).

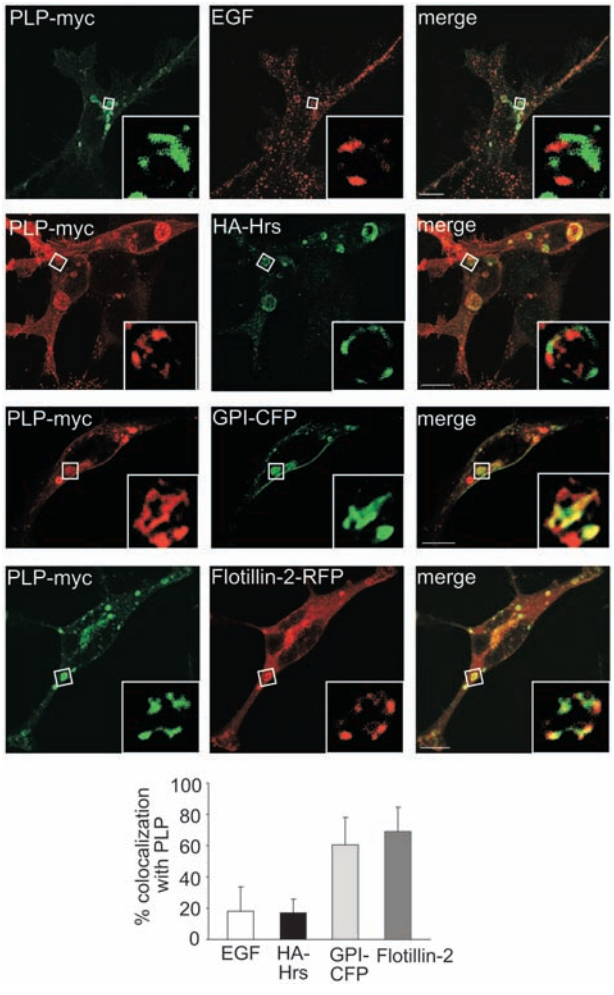

Fig. 2. Endosomal subdomain structure. Oli-neu cells were cotransfected with Rab5^{Q79L} and PLP-Myc, EGFR, hemagglutinin (HA) epitope–tagged Hrs (HA-Hrs), GPI-CFP, or flotillin-2 fused with red fluorescent protein (flotillin-2–RFP) as indicated. Cells transfected with EGFR were incubated for 15 min with rhodamine-labeled EGF. Cells were then processed and analyzed for immunofluorescence microscopy. The white box indicates the (inset) region reimaged in higher resolution and contrast to resolve the subdomain structure. Quantification of colocalization of the different proteins on endosome membranes is shown (n = ~25 endosomes). Scale bar, 10 μm.

We next addressed whether EGFR or PLP uses distinct pathways of inward budding into endosomes. Sorting of EGFR into ILVs requires the sequential action of different components of the ESCRT (endosomal sorting complex required for transport) machinery (*12*, *13*). To interfere with the function of the ESCRT machinery, we used either RNA interference (RNAi) or dominant-negative mutants against Hrs, Tsg101, Alix, or Vps4. Depletion of either Hrs or Tsg101 significantly reduced the intraluminal transport of EGF into enlarged endosomes, whereas Alix depletion only had a minor effect (fig. S4). The reduction of EGF in the endosomal lumen correlated with a defect in EGF degradation (fig. S5) (*13*). We also analyzed the effect of the Tsg101 depletion (knockdown) on intraendosomal transport of vesicular stomatitis virus G (VSV-G) to investigate ligand-independent transport. Depletion of Tsg101 reduced the amount of VSV-G within the lumen of the endosomes (fig. S6).

In contrast, knockdown of Hrs, Tsg101, or Alix had no influence on the inward budding of PLP (fig. S4). In addition, the functional inhibition of the ESCRT machinery did not change the colocalization of PLP with Lamp-1 (fig. S7). Thus, the pathway for intraendosomal transport of PLP may be ESCRT-independent. Furthermore, neither knockdown of Tsg101 and Alix nor expression of a dominant-negative Vps4 impaired the secretion of PLP with exosomes (fig. S8). Likewise, the release of CD63 (with enhanced GFP fusion, EGFP-CD63) was not affected by coexpression with dominant-negative Vps4 (fig. S9). Secretion of Gag-YFP with virus-like particles was strongly reduced by the expression of dominant-negative Vps4 (fig. S7) (*14*). In addition, overexpression of Tsg101, which inhibits HIV-1 budding (*15*), did not affect exosome release of PLP (fig. S10). Thus, PLP is transferred

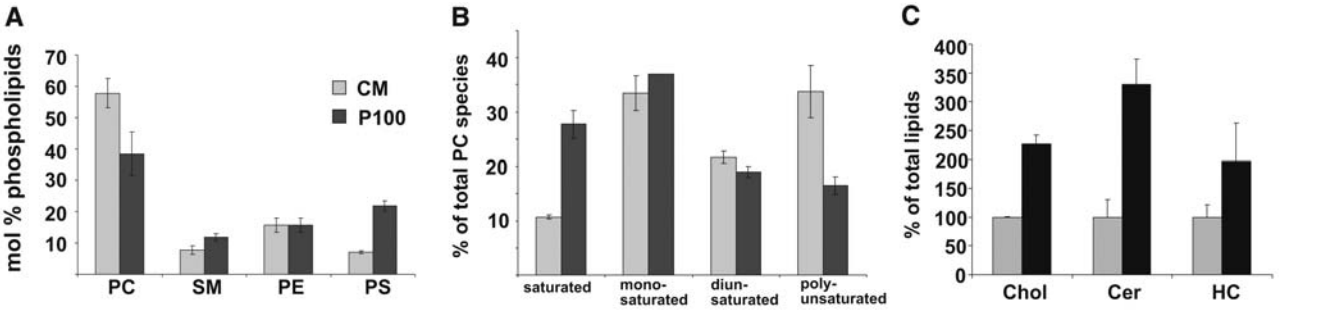

Fig. 3. Lipid analysis of exosomes. Analysis of (**A**) phospholipid classes, (**B**) PC composition, and (**C**) ratios of individual lipid classes from total cellular membranes (CM) and the exosome fractions (P100). The data are from three independent experiments; values are means ± SD. Chol, cholesterol; HC, hexosylceramide; Cer, ceramide; PE, phosphatidylethanolamine; and PS, phosphatidylserine.

into the lumen of endosomes and released with exosomes in an ESCRT-independent fashion.

To get insight into the ESCRT-independent budding machinery, we used nano-electrospray ionization tandem mass spectrometry to examine the molecular composition of exosomes. The lipid composition was remarkably similar to that of lipid rafts (*16*, *17*). Exosomes not only were enriched in cholesterol but also contained higher amounts of sphingolipids [sphingomyelin (SM) and hexosylceramide] and lower amounts of phosphatidylcholine (PC) than total cellular membrane (Fig. 3A). In addition, quantitative analysis of lipid molecular species revealed an increase in saturated PC, at the expense of polyunsaturated species in exosomes (Fig. 3B and fig. S11). Most important, we found a marked enrichment of ceramide in exosomes (Fig. 3C). Ceramide is formed after the hydrolytic removal of the phosphocholine moiety of SM by sphingomyelinases (SMases) (*18*). Exogenous SMase treatment or application of C_6-ceramide can induce the formation of vesicles (*19*–*21*). To analyze the role of ceramide in exosome biogenesis and release, we treated Oli-neu cells with the neutral sphingomyelinase (nSMase) inhibitor, GW4869. Exosome release was markedly reduced after treatment with GW4869 (Fig. 4, A and B, and fig. S9). The effect was also observed after treatment with the two structurally unrelated nSMase inhibitors, spiroepoxide and glutathione (Fig. 4, A and B). Furthermore, depletion of neutral sphingomyelinase 2 (nSMase2) with RNAi reduced the release of PLP but not Gag with exosomes. Next, we studied the effect of nSMase inhibition in intraendosomal transport of PLP. After treatment with GW4869, a significant reduction of the amount of PLP within the endosomal lumen was observed (Fig. 4B). This was not due to an unspecific derangement of the endosomal system, because the amount of intraendosomal VSV-G remained unchanged (Fig. 4, C and D) and because the degradation of EGF was not impaired (fig. S12). Furthermore, a reduction of PLP within the endosomal lumen was also observed after depletion of nSMase2 using RNAi (Fig. 4, C and D).

To further explore the role of ceramide in the formation of intravesicular membrane, we performed experiments using giant unilamellar vesicles (GUVs). We used a mixture of dioleoylphosphatidylcholine (DOPC), SM, and cholesterol to generate vesicles with two different lipid phases. 1,1′-Dioctadecyl-3,3,3′,3′-tetramethylindodicarbocyanine perchlorate (DiD-C18) and cholesterol with dipyrromethene boron difluoride (Bodipy-cholesterol) were used to mark the liquid-disordered and liquid-ordered (raftlike) lipid phases, respectively. We added SMase exogenously to these GUVs to analyze whether intravesicular membranes were formed from one of these lipid phases. Shortly after the addition of the SMase, small vesicles started to bud from the liquid-ordered lipid phase and to accumulate in the lumen of the GUVs (Fig. 4E). The intravesicular membrane was predominantly labeled by Bodipy-cholesterol and contained only small amounts of DiD-C18 (Fig. 4E).

Together, these data provide evidence for an alternative pathway for sorting cargo into MVEs, which is independent of the ESCRT machinery but seems to depend on raft-based microdomains for the lateral segregation of cargo within the endosomal membrane. These microdomains may contain high concentrations of sphingolipids from which ceramides are formed. Ceramide can induce the coalescence of small microdomains into larger domains, which promotes domain-induced budding (*22*). In addition, the cone-shaped structure of ceramide might induce

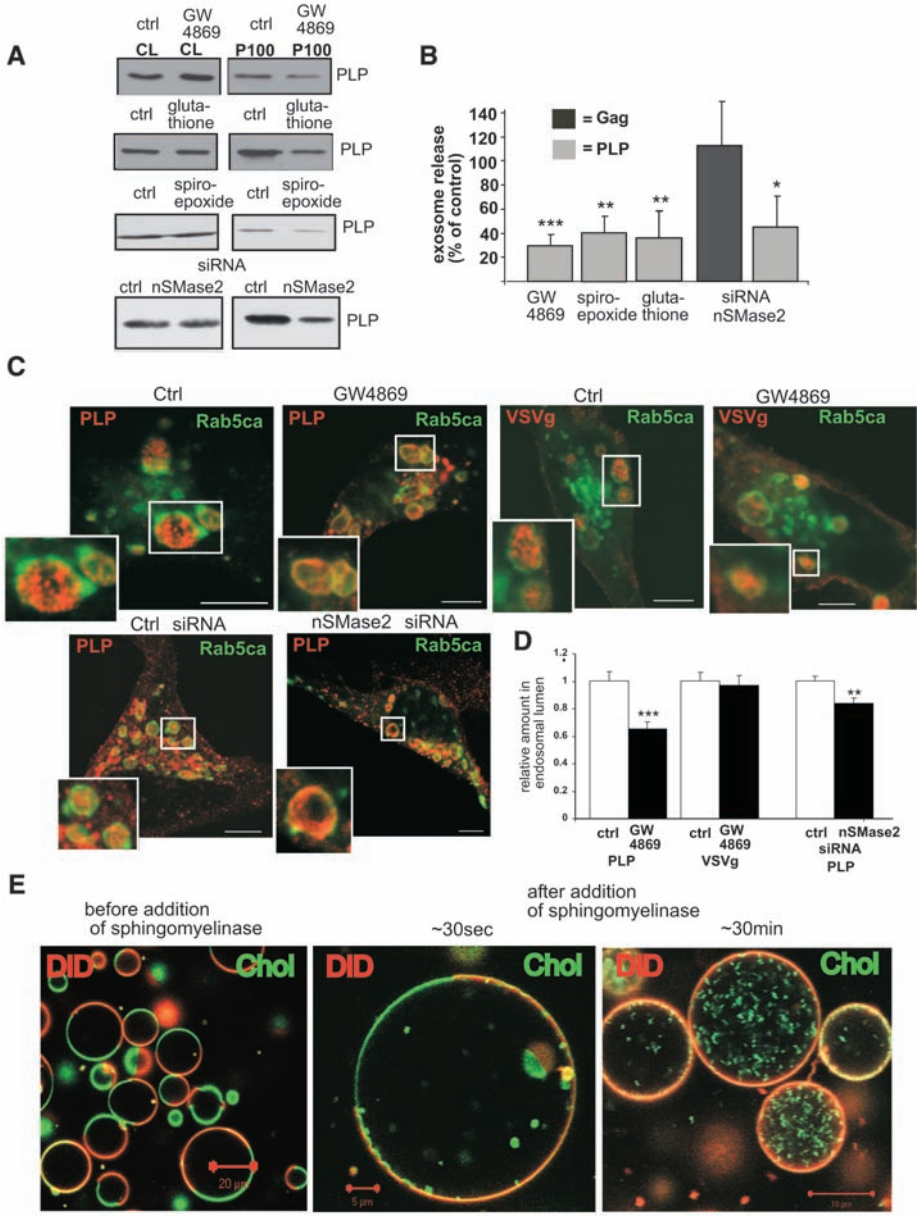

Fig. 4. Ceramide in the formation of intravesicular membrane and exosome release. (**A**) Oli-neu cells stably expressing PLP-EGFP were treated with 5 μM GW4869, 5 μM spiroepoxide, or 5 mM glutathione or with the respective vehicle. nSMase2 small interfering RNA (siRNA) was delivered by nucleofection into the cells. The amount of PLP-EGFP and Gag-YFP was determined in the cell lysates (CL) and in the exosome fractions (P100). (**B**) Results are expressed as means ± SD of three to six experiments (*$P < 0.05$; **$P < 0.01$; ***$P < 0.001$; one-sample t test against 100%). (**C**) Cells were treated as indicated and cotransfected with GFP-Rab5^{Q79L} and PLP-Myc or VSV-G and then processed and analyzed by immunofluorescence microscopy. (**D**) The amount of PLP or VSV-G in the endosomal lumen was quantified (fluorescence intensity in the lumen versus the limiting membrane; normalized to 1 for the controls). Values represent means ± SE ($n > 40$ endosomes; **$P < 0.01$, ***$P < 0.001$; t test). Scale bar, 5 μm. (**E**) GUVs were prepared with a mixture of DOPC, SM, and cholesterol. DiD-C18 (red) and Bodipy-cholesterol (green) were used to mark the two lipid phases. GUVs were incubated with SMase from *Staphylococcus aureus*. Confocal pictures are shown before and at two different time points after the addition of SMase, as indicated.

spontaneous negative curvature by creating an area difference between the membrane leaflets. Another cone-shaped lipid, lysobisphosphatidic acid, induces the formation of internal vesicles in liposomes (*23*). This lipid, which is absent from exosomes (*16*), may regulate biogenesis and dynamics of ILVs along the degradative pathway (*24*). Ceramide, in contrast, seems to be used for the generation of another population of ILVs that are not destined for transport to the lysosomes but are secreted as one class of exosomes.

References and Notes

1. R. C. Piper, D. J. Katzmann, *Annu. Rev. Cell Dev. Biol.* **23**, 519 (2007).
2. J. Gruenberg, H. Stenmark, *Nat. Rev. Mol. Cell Biol.* **5**, 317 (2004).
3. C. Thery, L. Zitvogel, S. Amigorena, *Nat. Rev. Immunol.* **2**, 569 (2002).
4. W. Stoorvogel, M. J. Kleijmeer, H. J. Geuze, G. Raposo, *Traffic* **3**, 321 (2002).
5. G. van Niel, I. Porto-Carreiro, S. Simoes, G. Raposo, *J. Biochem.* **140**, 13 (2006).
6. K. Trajkovic *et al.*, *J. Cell Biol.* **172**, 937 (2006).
7. A. de Gassart, C. Geminard, B. Fevrier, G. Raposo, M. Vidal, *Blood* **102**, 4336 (2003).
8. B. Fevrier *et al.*, *Proc. Natl. Acad. Sci. U.S.A.* **101**, 9683 (2004).
9. H. Stenmark *et al.*, *EMBO J.* **13**, 1287 (1994).
10. C. Raiborg *et al.*, *Nat. Cell Biol.* **4**, 394 (2002).
11. C. Raiborg, J. Wesche, L. Malerod, H. Stenmark, *J. Cell Sci.* **119**, 2414 (2006).
12. J. H. Hurley, S. D. Emr, *Annu. Rev. Biophys. Biomol. Struct.* **35**, 277 (2006).
13. R. L. Williams, S. Urbe, *Nat. Rev. Mol. Cell Biol.* **8**, 355 (2007).
14. J. E. Garrus *et al.*, *Cell* **107**, 55 (2001).
15. R. Goila-Gaur, D. G. Demirov, J. M. Orenstein, A. Ono, E. O. Freed, *J. Virol.* **77**, 6507 (2003).
16. R. Wubbolts *et al.*, *J. Biol. Chem.* **278**, 10963 (2003).
17. B. Brügger *et al.*, *Proc. Natl. Acad. Sci. U.S.A.* **103**, 2641 (2006).
18. C. J. Clarke *et al.*, *Biochemistry* **45**, 11247 (2006).
19. J. M. Holopainen, M. I. Angelova, P. K. Kinnunen, *Biophys. J.* **78**, 830 (2000).
20. X. Zha *et al.*, *J. Cell Biol.* **140**, 39 (1998).
21. R. Li, E. J. Blanchette-Mackie, S. Ladisch, *J. Biol. Chem.* **274**, 21121 (1999).
22. E. Gulbins, R. Kolesnick, *Oncogene* **22**, 7070 (2003).
23. H. Matsuo *et al.*, *Science* **303**, 531 (2004).
24. F. G. van der Goot, J. Gruenberg, *Trends Cell Biol.* **16**, 514 (2006).

25. We are grateful to R. Bittman, D. Caplan, M. Zerial, D. Arndt-Jovin, U. Coskun, P. Keller, D. Cutler, P. Burfeind, and H. Stenmark for providing reagents and R. White for help with RNAi experiments. The work was supported by the Deutsche Forschungsgemeinschaft (SFB 523, GRK521).

Supporting Online Material

www.sciencemag.org/cgi/content/full/319/5867/1244/DC1
Materials and Methods
SOM Text
Figs. S1 to S12
References

19 November 2007; accepted 8 January 2008
10.1126/science.1153124

Membrane Proteins of the Endoplasmic Reticulum Induce High-Curvature Tubules

Junjie Hu,[1] Yoko Shibata,[1] Christiane Voss,[2] Tom Shemesh,[3] Zongli Li,[4] Margaret Coughlin,[5] Michael M. Kozlov,[3] Tom A. Rapoport,[1]* William A. Prinz[2]*

The tubular structure of the endoplasmic reticulum (ER) appears to be generated by integral membrane proteins, the reticulons and a protein family consisting of DP1 in mammals and Yop1p in yeast. Here, individual members of these families were found to be sufficient to generate membrane tubules. When we purified yeast Yop1p and incorporated it into proteoliposomes, narrow tubules (~15 to 17 nanometers in diameter) were generated. Tubule formation occurred with different lipids; required essentially only the central portion of the protein, including its two long hydrophobic segments; and was prevented by mutations that affected tubule formation in vivo. Tubules were also formed by reconstituted purified yeast Rtn1p. Tubules made in vitro were narrower than normal ER tubules, due to a higher concentration of tubule-inducing proteins. The shape and oligomerization of the "morphogenic" proteins could explain the formation of the tubular ER.

How the characteristic shape of an organelle is generated and maintained is largely unknown. The endoplasmic reticulum (ER), for example, consists of continuous membrane sheets and tubules (*1*, *2*), but it is unclear how these domains are made and kept morphologically distinct. The tubules are interconnected in a polygonal network and have diameters ranging from ~30 nm in *Saccharomyces cerevisiae* (*3*) to ~50 nm in mammals (*4*). The most plausible models for shaping ER tubules are based on mechanisms that generate or stabilize the high membrane curvature seen in cross sections. A curvature-stabilizing role has been suggested for a class of integral membrane proteins, the reticulons and a protein family that includes DP1 in mammals and Yop1p in yeast (*5*). These proteins are found in most, if not all, eukaryotic cells. They form homo- and heterooligomers and localize exclusively to ER tubules. Their overexpression generates long, unbranched tubules, and their deletion in yeast leads to the loss of tubular ER. The reticulon and Yop1p (DP1) families are not related in sequence, but they each contain a conserved domain of ~200 amino acids that includes two hydrophobic segments, which seem to form a hairpin in the membrane. It remains unclear whether the reticulons or Yop1p (DP1) are sufficient for tubule formation and how they might deform the membrane.

[1]Howard Hughes Medical Institute and Department of Cell Biology, Harvard Medical School, 240 Longwood Avenue, Boston, MA 02115, USA. [2]Laboratory of Cell Biochemistry and Biology, National Institute of Diabetes and Digestive and Kidney Disorders (NIDDK), National Institutes of Health, Bethesda, MD 20892, USA. [3]Department of Physiology and Pharmacology, Sackler Faculty of Medicine, Tel Aviv University, Ramat Aviv, 69978 Tel Aviv, Israel. [4]Department of Cell Biology, Harvard Medical School, 240 Longwood Avenue, Boston, MA 02115, USA. [5]Department of Systems Biology, Harvard Medical School, 240 Longwood Avenue, Boston, MA 02115, USA.

*To whom correspondence should be addressed. E-mail: tom_rapoport@hms.harvard.edu (T.A.R.); wprinz@helix.nih.gov (W.A.P.)

We first tested whether the reticulon and Yop1p (DP1) proteins would each generate membrane tubules when reconstituted with lipids into proteoliposomes. Yop1p was purified from *S. cerevisiae* with a cleavable N-terminal histidine (His) tag in the detergent lauryldimethylamine-*N*-oxide (LDAO) (Fig. 1A) (*6*). After cleavage of the His tag, *Escherichia coli* polar lipids were added, and the detergent was removed with Biobeads to generate proteoliposomes. At early time points during the reconstitution reaction, small vesicles and short tubules were seen by negative-stain electron microscopy (EM), both with a diameter of ~17 nm (Fig. 1B). Over the course of a day, the vesicles disappeared and the tubules grew in length, reaching several hundred nanometers, but their diameter remained the same (Fig. 1C). The tubules occasionally had branch points (Fig. 1C), which indicated that the lipid bilayers could branch or fuse during reconstitution. No tubules were seen when the lipids were omitted (Fig. 1D). In the absence of protein, round liposomes with heterogeneous size were generated (Fig. 1E). Yop1p formed tubules of identical diameter when reconstituted with other lipids (fig. S1), which suggested that the protein was primarily responsible for the shape of the proteoliposomes.

Next, we tested whether yeast reticulon Rtn1p could also induce tubules in vitro. Tubules were indeed seen in negative-stain EM when purified Rtn1p (Fig. 1F) was mixed with *E. coli* polar lipids and the detergent was removed by dialysis (Fig. 1G). The diameter of these tubules was about the same as with Yop1p, but bulges were frequently observed. When the detergent was removed by Biobeads, Rtn1p tubules were not generated, whereas, with Yop1p, both Biobeads and dialysis resulted in tubule formation. Because Rtn1p was less efficient than Yop1p in forming tubules, most of the subsequent experiments were performed with Yop1p.

Increasing the lipid concentration or decreasing the protein concentration in the reconstitution reaction resulted in fewer Yop1p tubules and an increased number of large vesicles (table

ERRATUM

Post date 11 April 2008

Reports: "Ceramide triggers budding of exosome vesicles into multivesicular endosomes" by K. Trajkovic *et al*. (29 February, p. 1244). Two papers on ESCRT-independent transport should have been cited on page 1245. The text beginning "the pathway for intraendosomal transport of PLP may be ESCRT-independent" should continue "similar to the transport of Pmel17 into melanosomes" and cite A. C. Theos *et al*., *Dev. Cell* **10**, 343 (2006). The text beginning "the release of CD63 (with enhanced GFP fusion, EGFP-CD63) was not affected by coexpression with dominant-negative Vps4 (fig. S9)" should continue "as shown previously" and cite Y. Fang *et al*., *PLoS Biol*. **5**, e158 (2007).

Ceramide Triggers Budding of Exosome Vesicles into Multivesicular Endosomes

Katarina Trajkovic, Chieh Hsu, Salvatore Chiantia, Lawrence Rajendran, Dirk Wenzel, Felix Wieland, Petra Schwille, Britta Brügger and Mikael Simons

Science **319** (5867), 1244-1247.
DOI: 10.1126/science.1153124